Structural and functional recovery from early monocular deprivation in adult rats

Tommaso Pizzorusso*†‡§, Paolo Medini‡¶‖, Silvia Landi¶, Sara Baldini¶, Nicoletta Berardi*†, and Lamberto Maffei*¶

*Istituto di Neuroscienze, Consiglio Nazionale delle Ricerche, Via Moruzzi 1, 56100 Pisa, Italy; †Dipartimento di Psicologia, Università di Firenze, 50123 Firenze, Italy; and ¶Scuola Normale Superiore, 56100 Pisa, Italy

Communicated by Emilio Bizzi, Massachusetts Institute of Technology, Cambridge, MA, March 31, 2006 (received for review December 15, 2005)

Visual deficits caused by abnormal visual experience during development are hard to recover in adult animals. Removal of chondroitin sulfate proteoglycans from the mature extracellular matrix with chondroitinase ABC promotes plasticity in the adult visual cortex. We tested whether chondroitinase ABC treatment of adult rats facilitates anatomical, functional, and behavioral recovery from the effects of a period of monocular deprivation initiated during the critical period for monocular deprivation. We found that chondroitinase ABC treatment coupled with reverse lid-suturing causes a complete recovery of ocular dominance, visual acuity, and dendritic spine density in adult rats. Thus, manipulations of the extracellular matrix can be used to promote functional recovery in the adult cortex.

amblyopia | chondroitin sulfate | extracellular matrix | glycosaminoglycan | plasticity

An abnormal visual experience during development results in defective visual function. For instance, cataract or anisometropia in early childhood leads to a condition of reduced visual acuity (amblyopia) that can be fully recovered only if the treatment of these conditions is performed during early infancy (1). The lack of substantial recovery from amblyopia in the adult has been attributed to a decline in the plasticity of cortical circuits occurring during late postnatal development. Indeed, studies in animals have shown that monocular deprivation (MD) impairs visual cortical responses to the deprived eye and affects axonal morphology and dendritic spine density only if performed during a critical period of postnatal development (2–6). The ability to recover from the deficits induced by MD declines with age; reopening the previously deprived eye or reverse lid-suturing (RS) in young animals results in full recovery of ocular dominance, but these procedures become progressively less effective with age and are practically ineffective in the adult (7–9). Recovery from the amblyopic effect of MD is also progressively less efficient during development. In the adult, visual acuity shows small recoveries even if its final level continues to be pathologically low (10, 11). Similarly, a limited recovery of visual acuity can also be observed in adult amblyopic patients in particular conditions (1), although visual acuity remains largely abnormal.

These observations suggest that the adult visual cortex expresses factors that inhibit experience-dependent plasticity and that develop in conjunction with the end of the critical period. The molecular identity of these factors is only partially known (12); studies performed in rodents have attributed the closure of the critical period to the maturation of inhibitory intracortical circuitry (13, 14) and to developmental changes in the expression of molecular factors regulating synaptic plasticity (15, 16). Recently, it has been shown that at least part of the low level of plasticity of the adult visual cortex is due to the condensation of extracellular matrix molecules in perineuronal nets (PNNs). Indeed, chondroitinase ABC (chABC) treatment of the adult rat visual cortex, which removes crucial components of PNNs such as chondroitin sulfate proteoglycans (CSPGs), reactivates sensitivity to MD after the end of the critical period (17).

If the weak plasticity present in the visual cortex at the end of the critical period is responsible for the weak recovery from MD in the adult, chABC, which is capable of reactivating ocular dominance plasticity, should also promote recovery from the functional and anatomical effects of long-term MD in the adult. This hypothesis was tested by analyzing whether chABC can promote recovery of ocular dominance, visual acuity, and spine density after RS of long-term MD adult rats.

Results

RS Causes a Limited Spontaneous Recovery of Ocular Dominance in Adult Rats. We initially studied the extent of spontaneous functional recovery possibly occurring in adult untreated MD rats. Rats were MD at postnatal day 21 (P21) and were subjected to RS well after the end of the rat critical period for MD (age, P120–P300; median, P160). After 7 days of RS, we assessed ocular dominance distribution by means of single-unit recordings from the binocular field of the primary visual cortex contralateral to the deprived eye. Ocular dominance was quantitatively attributed to each unit on the basis of the computer-acquired response to visual stimulation of either eye according to a modified Hubel and Wiesel classification (2) and by assigning to each neuron a normalized ocular dominance score.

As shown in Fig. 1*A*, the ocular dominance distribution of the animals subjected to RS after long-term MD remained significantly shifted toward the eye that was open during the first period of MD, although this shift was attenuated compared with MD rats recorded immediately after eye opening. The minimal recovery of ocular dominance by RS in adult MD rats was confirmed by analyzing the cumulative distribution of the normalized ocular dominance score, which allows a finer and more robust statistical comparison (Fig. 1*B*; Kolmogorov–Smirnov test, $P < 0.05$), and by studying interindividual variability of ocular dominance by computing a contralateral bias index (CBI) (17) for each animal (Fig. 1*C*). To analyze whether recovery could be specifically present in specific cortical layers, we subdivided the cells into three classes [superficial, 0–500 μm; intermediate, 500–650 μm; and deep, >650 μm, corresponding to layers II–III, IV, and V–VI, respectively (18)] according to their depth in the cortex. Computing ocular dominance distribution for each class, we found some spontaneous recovery in all classes, although statistical significance ($P < 0.05$; χ^2 test) was reached only in superficial and deep layers.

Conflict of interest statement: No conflicts declared.

Abbreviations: chABC, chondroitinase ABC; CBI, contralateral bias index; CSPG, chondroitin sulfate proteoglycan; MD, monocular deprivation/monocularly deprived; P*n*, postnatal day *n*; PNN, perineuronal net; RS, reverse lid-suturing/reverse lid-sutured; VEP, visually evoked potential; WFA, *Wisteria floribunda* agglutinin lectin; P-ase, penicillinase.

‡T.P. and P.M. contributed equally to this work.

§To whom correspondence may be addressed at: Istituto Neuroscienze, Consiglio Nazionale delle Ricerche, Via Moruzzi 1, 56100 Pisa, Italy. E-mail: tommaso@in.cnr.it.

‖To whom correspondence may be addressed. E-mail: medini@in.cnr.it.

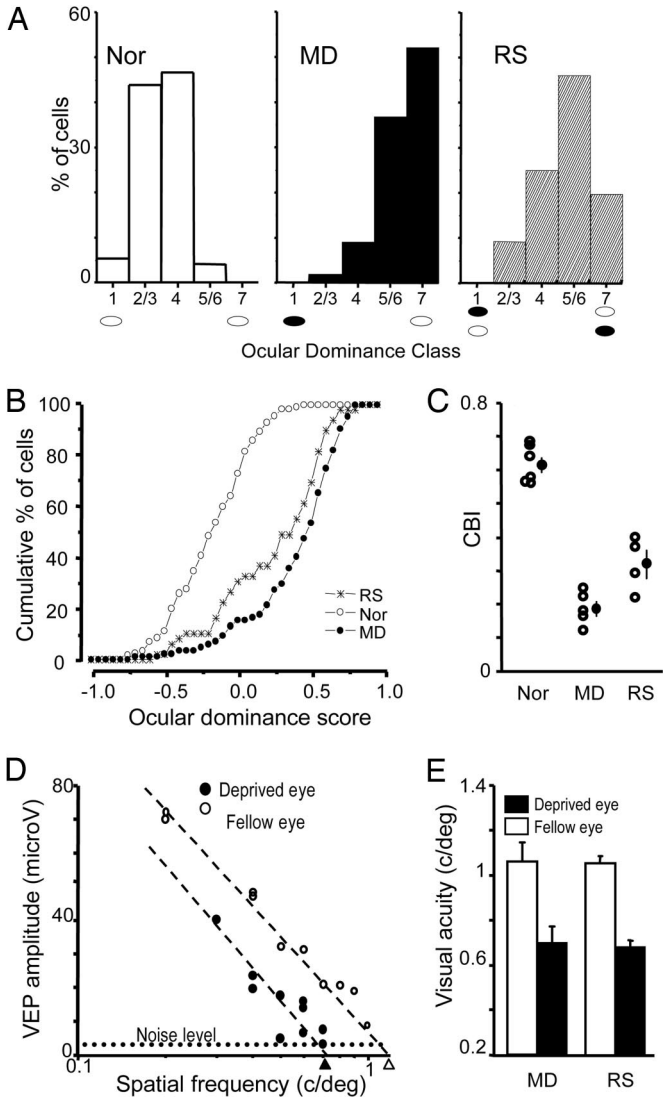

Fig. 1. Persistence of MD effects in adult RS rats. (*A*) The ocular dominance of visual cortical neurons remains shifted toward the previously nondeprived eye in adult RS rats. Ocular dominance distributions of nondeprived [normal (Nor); $n = 6$; 149 cells], long-term MD (MD; $n = 5$; 95 cells), and RS (RS; $n = 4$; 80 cells) rats significantly differ from each other (χ^2 test, $P < 0.05$). (*B*) Ocular dominance score distributions of Nor, MD, and RS rats (Kolmogorov–Smirnov test, $P < 0.05$). (*C*) CBIs (open circles, values of single animals; filled circles, mean ± SE) of Nor, MD, and RS rats (one-way ANOVA, $P < 0.001$; all groups differ form each other; post hoc Tukey test, $P < 0.05$). (*D*) Representative example of visual acuity estimates of both eyes in an RS animal. VEP transient amplitude is plotted against the spatial frequency log. Visual acuity is taken as the spatial frequency that coincides with the extrapolation to zero amplitude of the linear regression through the last four to five data points above noise level. Dashed lines indicate noise level. (*E*) The visual acuity of the formerly deprived eye is significantly lower than that of the other eye in both MD and RS adult rats (paired *t* test, $P < 0.05$). Visual acuity of the other eye was within the normal acuity values estimated with VEPs or behaviorally in the rat.

Lack of Spontaneous Recovery of Visual Acuity of the Long-Term-Deprived Eye in Adult RS Rats. We then asked whether RS could recover the reduction of visual acuity caused by MD (1, 19). In the same animals used for ocular dominance assessment, we estimated visual acuity of either eye by means of visually evoked potential (VEP) recordings from the same cortical location used for single-unit recordings. VEP visual acuity measures are in agreement with behavioral estimates in all species tested so far, including humans. A representative example of the visual acuity estimate of the two eyes of an RS rat is shown in Fig. 1*D*. The average visual acuity of the long-term-deprived eye after 1 week of RS was significantly lower than that of the other eye and was not different from visual acuity of the deprived eye of long-term MD rats without RS (Fig. 1*E*). Visual acuity of the other eye was within the normal acuity values estimated with VEPs or behaviorally in the rat (11, 19). Thus the amblyopic effects of MD are not rescued by 1 week of RS.

chABC Promotes Recovery of Normal Ocular Dominance and Receptive Field Size of Cortical Neurons. The persistence of the effects of MD in adult RS rats makes it possible to use this model to test whether treatments that reactivate ocular dominance plasticity in the adult rat can be exploited to promote recovery from MD effects. We have shown previously that ocular dominance plasticity can be reactivated in the adult by cortical administration of chABC, a bacterial enzyme that digests the lateral glycosaminoglycan chains of CSPGs. This treatment does not cause detrimental effects on neuronal or glial survival, alterations of visual acuity, or abnormalities of receptive field size and spiking activity, either spontaneous or visually evoked, of visual cortical neurons (17). Therefore, we studied whether chABC treatment can promote recovery from the effects of long-term MD in the adult.

Long-term MD animals were RS for 1 week and concurrently subjected to intracortical injections of protease-free chABC or penicillinase (P-ase, a bacterial enzyme without endogenous substrates) as a control. chABC or P-ase was administered in the cortex contralateral to the eye subjected to the long-term MD. In all animals, glycosaminoglycan chain removal by chABC was controlled by histochemistry on fixed slices by using a biotinylated *Wisteria floribunda* agglutinin lectin (WFA) that binds to CSPG glycosaminoglycans. As shown in the examples in Fig. 2 *A* and *B*, chABC treatment, but not P-ase treatment, completely removed WFA staining. Complete glycosaminoglycan digestion was observed in the visual cortex of all of the chABC-treated rats.

Single-unit recordings from the RS animals treated with chABC showed that the ocular dominance distribution was completely recovered and took the shape typical of the ocular dominance distribution of normal animals (Fig. 2*A*). The distribution of the control RS plus P-ase-treated animals was not statistically different from that of RS untreated animals (Fig. 2*B*). These data were confirmed by analyzing the cumulative distribution of the ocular dominance score for each experimental group (Fig. 2*C*). CBIs of single chABC-treated animals also fell in the normal range, showing that recovery of eye dominance is present in all chABC-treated rats (Fig. 2*D*). Subdividing recorded cells according to their depth in superficial, intermediate, and deep cortical layers, we found that ocular dominance distribution was significantly recovered in all layers (χ^2 test, $P < 0.01$).

Long-term MD also affects receptive field size (20). We measured unit receptive field size on peristimulus time histograms elicited by stimulation of the contralateral eye in normal rats, control RS rats, and RS rats treated with chABC. Receptive field size differed across these groups (Kruskal–Wallis one-way ANOVA, $P = 0.005$). Receptive field size of the contralateral, long-term-deprived eye of control rats (median, 17.9°; 25th to 75th percentile, 11.8–25.0°; $n = 94$ cells) was significantly larger than that of normal rats (median, 13.4°; 25th to 75th percentile, 8.3–19.1°; $n = 133$ cells; post hoc Dunn's test, $P < 0.05$). This effect of MD was largely recovered by chABC; indeed, receptive field size of the long-term-deprived eye in chABC-treated rats was not different from normal values (median, 15°; 25th to 75th percentile, 10.2–21.2°; $n = 173$ cells; post hoc Dunn's test, $P > 0.05$). These results show that CSPG removal in the adult visual cortex coupled with RS allows a complete recovery of ocular

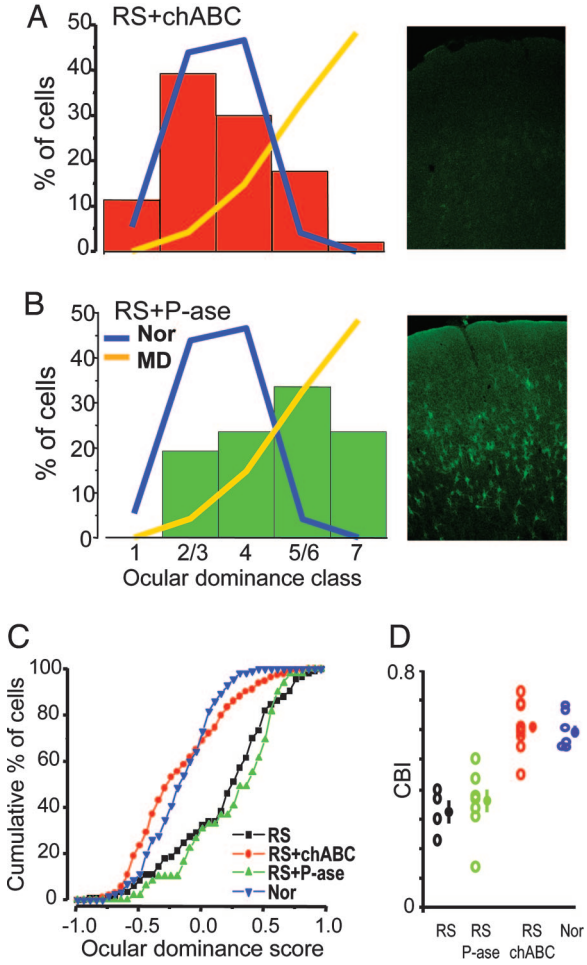

Fig. 2. chABC treatment allows complete recovery of ocular dominance in adult RS rats. (*A Left*) Ocular dominance distribution of RS chABC-treated (RS+chABC; $n = 9$; 204 cells) rats is statistically undistinguishable from that of adult normal rats (χ^2 test, $P > 0.05$). (*A Right*) Perineuronal and diffuse WFA staining is completely abolished in visual cortex of recorded chABC-treated animals. (*B Left*) Ocular dominance distribution of adult RS P-ase-treated (RS+P-ase; $n = 7$; 140 cells) rats remains significantly shifted toward the previously deprived eye. For comparison, the distribution of normal adults (Nor, blue line) and long-term MD rats (MD, orange line) reported in Fig. 1 is outlined. Data for the Nor and MD groups are the same as those in Fig. 1. (*B Right*) Normal appearance of CSPG-containing PNNs stained with WFA in a recorded rat treated with P-ase (field centered on layer 4). (*C*) The ocular dominance score distribution of RS+chABC animals is significantly shifted toward normal values with respect to both the RS and RS+P-ase groups. The RS and RS+P-ase groups do not differ between themselves (Kolmogorov–Smirnov statistics, level of significance of 0.05). (*D*) CBIs (open circles, values of single animals; filled circles, mean ± SE) of RS, RS+P-ase, RS+chABC, and Nor rats. Statistical analysis shows that CBIs of RS+chABC rats are not different from those of normal rats but differ from CBIs of RS and RS+P-ase rats (one-way ANOVA, level of significance $P = 0.001$; all groups differ from each other; post hoc Tukey test, level of significance $P = 0.05$).

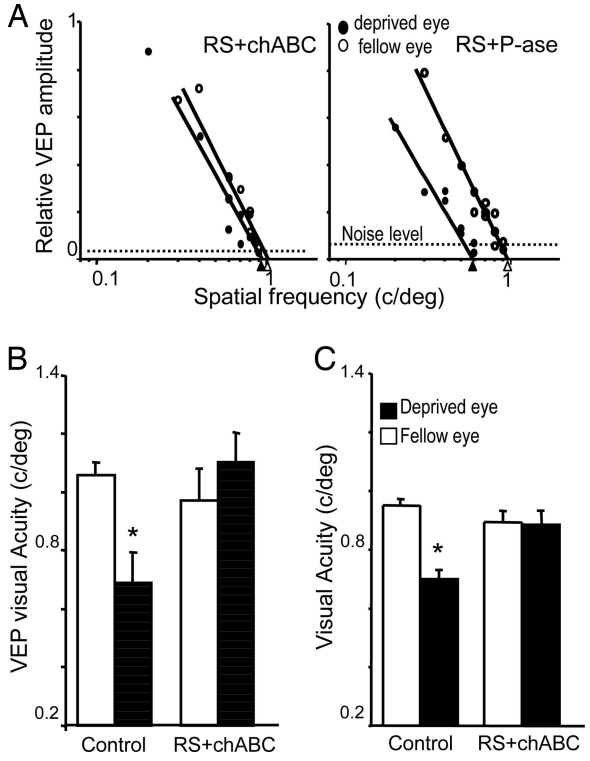

Fig. 3. chABC causes a complete recovery of visual acuity of the previously deprived eye. (*A*) Representative examples of visual acuity assessment of the previously deprived and nondeprived eyes in two rats treated with P-ase (*Right*) and chABC (*Left*) after 1 week of RS. VEP amplitude is normalized to peak amplitude. (*B*) Visual acuity of the two eyes in both experimental groups. Statistical analysis confirms that the treatment with chABC promoted a complete recovery of visual acuity of the formerly deprived eye (paired *t* test, level of significance of 0.05). (*C*) Behavioral visual acuity of a normal eye (open bar) and long-term-deprived eye (filled bar) of control animals [$n = 4$ (two P-ase rats and two untreated rats)] and chABC-treated animals ($n = 4$). Paired *t* test shows that visual acuity of the long-term-deprived eye is significantly reduced with respect to the normal eye in controls but not in chABC-treated animals. Asterisks in *B* and *C* indicate statistically different groups.

dominance and receptive field size of the previously long-term-deprived, contralateral eye.

chABC Promotes Recovery of Visual Acuity of the Long-Term-Deprived Eye: Electrophysiological and Behavioral Experiments. The effects of the chABC treatment on visual acuity were assessed by recording VEPs or by using a two-alternative forced-choice discrimination task (visual water box) (11). As shown in Fig. 3 *A* and *B*, VEP visual acuity of the formerly deprived eye was not different from that of the other eye in RS plus chABC animals. As expected, control P-ase treatment did not facilitate the recovery of visual acuity of the formerly closed eye: its visual acuity remained lower than that of the other eye. Acuity of the other eyes of the chABC- or P-ase-treated rats was in the normal range of acuity of the rat.

The recovery of visual acuity of the long-term-deprived eye that was observed by recording VEPs could also be observed behaviorally. Behavioral assessment began with the measurement of visual acuity of the open eye in long-term MD rats. Then RS was performed, and both visual cortices were treated with chABC or control. After 1 week, visual acuity of the long-term-deprived eye was assessed. We found that visual acuity of the long-term-deprived eye was at the level of the other eye in RS plus chABC animals. In contrast, the long-term-deprived eye of control rats remained amblyopic (Fig. 3*C*).

chABC Promotes the Experience-Dependent Recovery of Spine Density. In the visual cortex, altered spine number has been observed on apical dendrites of layer V or basal dendrites of layer III pyramidal neurons after prolonged dark rearing (21, 22). Recently, it has been found that MD also reduces spine density on layer II–III pyramidal neurons contralateral to the deprived eye, with this change being transient on distal parts of the dendrite and stable on its proximal segment (4). To assess whether the effects of chABC could be mediated by the activation of structural plasticity of dendritic spines, we measured spine

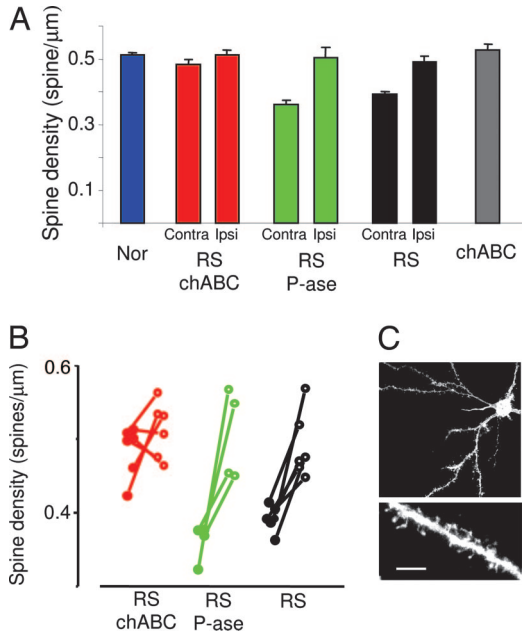

Fig. 4. chABC combined with RS causes a significant recovery of dendritic spine density. (*A*) Mean spine density in normal rats (Nor), RS rats, RS P-ase-treated rats (RS P-ase), RS chABC-treated rats (RS chABC), and nondeprived rats treated with chABC (chABC). The data of RS, RS P-ase, and RS chABC are reported separately for the cortex ipsilateral (Ipsi) to the long-term-deprived eye that is untreated and the cortex contralateral (Contra) to the long-term-deprived eye that is treated with chABC or P-ase. In both RS P-ase and RS rats, spine density in the cortex contralateral to the deprived eye is smaller than in normal rats. In contrast, spine density in RS chABC-treated rats did not differ from normal rats (one-way ANOVA, $P < 0.001$; post hoc Tukey test, Nor vs. RS and RS P-ase, $P < 0.001$; Nor vs. RS chABC, $P = 0.4$). Spine density in the cortex ipsilateral to the deprived eye was not different among groups (Nor, RS, RS P-ase, RS chABC; one-way ANOVA, $P = 0.82$). The chABC treatment *per se* does not affect spine density (chABC vs. Nor, $P = 0.42$, *t* test). (*B*) Within-animal comparison of spine density in RS, RS P-ase, and RS chABC. Data from single animals are reported. Filled circles represent data for the cortex contralateral to the long-term-deprived eye; open circles represent values for the cortex ipsilateral to the long-term-deprived eye. Data from the same animal are connected by a segment. In RS and RS P-ase, density is significantly smaller in the contralateral cortex (RS P-ase, $P = 0.037$; RS, $P = 0.003$; paired *t* test). No difference is present between the two cortices of RS chABC rats ($P = 0.29$, paired *t* test). (*C*) Example of a layer II–III pyramid cell of the binocular visual cortex and of a dendritic branch. (Scale bar in *C*: *Upper*, 40 μm; *Lower*, 5 μm.)

density on the proximal part [beginning at 26.2 μm (SD, 6.8) from the soma depending on primary dendrite morphology; length of analyzed segments, 31.9 μm (SD, 12)] of the basal dendrite of 1,1′-dioctadecyl-3,3,3′,3′-tetramethylindocarbocyanine-labeled layer II–III pyramids using "DiOlistic" staining (23). Long-term MD decreased spine density in the cortex contralateral to the deprived eye even after 1 week of RS when compared with normal animals or with the cortex ipsilateral to the deprived eye measured within the same sections (Fig. 4). It is likely that MD is more effective on spines of the cortex contralateral to the deprived eye than on spines of the ipsilateral cortex because of the conspicuous contralateral bias present in the retinogeniculate projection of rodents. As shown in Fig. 4 *A* and *B*, the decrease in spine density caused by long-term MD was recovered by chABC treatment. Indeed, spine density in the long-term-deprived cortex of RS rats treated with chABC was not different from spine density of normal rats or of the cortex ipsilateral to the deprived eye. The increase in spine density required the visual input originating from the reopened eye because chABC *per se* did not modify spine density in nondeprived rats (Fig. 4*B*).

Discussion

We showed that RS combined with treatment with chABC promotes complete recovery from the shift of ocular dominance preference of visual cortical neurons toward the formerly open eye and from the degradation of receptive field size caused by early MD. The loss of visual acuity of the formerly deprived eye is also recovered, as shown at electrophysiological and behavioral levels. This functional recovery is accompanied by significant recovery of dendritic spine density. These effects of the chABC treatment could involve the potentiation of forms of plasticity existing in the adult visual cortex such as the experience-dependent potentiation of visual responses recently observed in mice (24) or the reactivation of forms of plasticity present during the critical period and inhibited by CSPGs in the adult cortex. An indication of the mechanisms underlying the effects of chABC on recovery from the effects of MD comes from our data showing that reopening the formerly deprived eye recovers spine density to normal values in adult animals treated with chABC. *In vivo* two-photon imaging studies have shown that the adult visual cortex displays a remarkable level of structural stability, even at the level of single spines over a time course of months, which is in contrast to the anatomical rearrangements observed in the visual cortex during the critical period either in normal conditions or after binocular deprivation or MD (4, 5, 22, 25–28). This structural stability might be caused by the presence of factors in the extracellular matrix of the visual cortex exerting an inhibitory control over structural plasticity, as suggested by two recent studies that demonstrate that dynamic modifications of dendritic spines require extracellular proteolysis (4, 5). CSPGs are inhibitory for structural rearrangements and axonal sprouting and growth (29, 30), and they are extremely abundant in the extracellular matrix of the adult visual cortex (15, 17). Their removal from the adult extracellular matrix removes an obstacle for experience-dependent structural modifications, at least at the spine level. Thus, formation of synaptic contacts on the newly formed spines by the inputs from the formerly deprived eye might be the mechanism underlying the recovery from amblyopia observed in chABC-treated animals.

CSPG control of spine plasticity could be exerted directly by the CSPGs located around pyramidal neurons (15, 31). However, it is well known that toward the end of the critical period, CSPGs condense at an extremely high concentration in PNNs surrounding parvalbumin-positive inhibitory interneurons (32). This neuronal population has an important role in regulating the onset and offset of the critical period (13, 33), and a critical level of intracortical inhibitory tone also is required for experience-dependent plasticity of dendritic spines during the critical period (4). Therefore, at least some of the effects of chABC could be mediated by modifications of intracortical inhibitory circuits occurring after PNN degradation, which brings the status of parvalbumin interneurons back to the critical period (34).

The treatment with chABC has been shown to promote the plastic mechanisms underlying recovery from several forms of damage in the CNS. In particular, experiments in which the treatment of rat spinal cord injuries with chABC resulted in behavioral improvement (35) triggered a clinical interest in the use of chABC as a treatment for spinal cord injury in patients. Our data suggest that chABC might also be helpful in promoting recovery from amblyopia.

Experimental Procedures

Animal Treatment and Surgical Procedures. Rats were anesthetized with avertin (1 ml/hg) and mounted on a stereotaxic apparatus. MD was achieved by eyelid suturing at P21. For RS experiments, long-term MD animals with even minimal eye openings (observed with a surgical microscope) were excluded, and great care was taken to reopen the eye and to prevent opacities of the

reopened eye by topical application (twice daily) of antibiotic and cortisonic drops during the first 3 days of RS. Cortical microinjections of protease-free chABC or P-ase were done in concomitance with and 3 days after RS as described (17). Injections of 750 nl of a 48 units/ml solution of the two enzymes were made at five locations surrounding the rat primary visual cortex by means of a glass pipette (30-μm tip diameter) mounted on a motorized (0.1-μm step) three-axis micromanipulator connected to an injector. The five locations were, with respect to lambda: 3.8 mm lateral and 1 mm posterior, 3.8 mm lateral and 1 mm anterior, 6.2 mm lateral and 1 mm posterior, 6.2 mm lateral and 1 mm anterior, and 5 mm lateral and 2 mm anterior. For each location, 375 nl was released at two different depths (350 and 750 μm) to favor diffusion of the enzymes. The injection sites were at least 1 mm from the area in which recordings and histological assessments were performed. In all animals, the effectiveness of the treatment was controlled by WFA histochemistry as described (17).

We have shown previously that sensitivity to MD can be reactivated in the adult by cortical administration of chABC. This treatment is particularly suitable for promoting functional recovery from the effects of MD because previous experiments have shown that chABC treatment does not cause detrimental effects on neuronal or glial survival, alterations of visual acuity, or abnormalities of receptive field size and spiking activity, either spontaneous or visually evoked, of visual cortical neurons (17). As observed previously (36), the treatment with chABC did not alter the density of parvalbumin-positive neurons in visual cortex.

***In Vivo* Electrophysiology.** Animals were anesthetized with urethane (0.7 ml/hg; 20% solution in saline; Sigma) by i.p. injection and placed in a stereotaxic frame. Additional doses of urethane were used to keep the anesthesia level stable throughout the experiment. Body temperature was continuously monitored and maintained at ≈37°C by a thermostated electric blanket during the experiment. An ECG was continuously monitored. A hole was drilled in the skull, corresponding to the binocular portion of the primary visual cortex (binocular area Oc1B) contralateral to the long-term-deprived eye. After exposure of the brain surface, the dura was removed, and a micropipette (2 MΩ) filled with NaCl (3 M) was inserted into the cortex 5 mm from the central fissure. To prevent sampling bias, at least three well spaced penetrations were performed for each animal. Care was taken to equally sample cells across the entire cortical depth so that all layers contributed to the analysis of the ocular dominance and electrical activity.

Both eyes were fixed and kept open by means of adjustable metal rings surrounding the external portion of the eye bulb. Visual stimuli were hand-moved light bars projected on a reflecting tangent screen or computer-generated bars on a display (28×22 cm; 15 cd/m^2; Daewoo). Only cells with a receptive field within 20° from the vertical meridian were included in our sample. Care was taken that receptive fields were at comparable eccentricities in the different groups.

Quantitative Measure of the Main Cell-Response Properties. ***Cell responsiveness.*** Cell responsiveness was assessed according to standard criteria in terms of the amplitude of modulation of cell discharge in response to an optimal visual stimulus (peak response divided spontaneous discharge). Spontaneous discharge (spikes per second) was evaluated by a peristimulus time histogram over a period of 1–2 min during which the screen was kept at constant luminance. Peak response was evaluated as the peak firing rate (spikes per second) in the cell response to the stimulus averaged over 10–20 stimuli presentations. No difference of responsiveness was observed among the various groups of animals (RS: median, 7.8; 25th to 75th percentile, 5.1–9.9; RS plus P-ase: median, 8.8; 25th to 75th percentile, 5.6–15.4; RS plus chABC: median, 7.9; 25th to 75th percentile, 5.2–14.0; one-way ANOVA on ranks, $P = 0.23$).

Ocular dominance. Ocular dominance was evaluated according to a modified classification of Hubel and Wiesel (2). Cells in ocular dominance class 1 were neurons driven only by the contralateral eye, cells in ocular dominance classes 2 and 3 were binocular and preferentially driven by the contralateral eye (ratio of contralateral to ipsilateral peak response, >1.5), neurons in ocular dominance class 4 were equally driven by the two eyes, neurons in ocular dominance classes 5 and 6 were binocular and preferentially driven by the ipsilateral eye (ratio of ipsilateral to contralateral peak response, >1.5), and neurons in ocular dominance class 7 were driven only by the ipsilateral eye. In addition, to obtain a finer and statistically more robust comparison of ocular dominance distributions, we also computed for each neuron the normalized ocular dominance score of single neurons (37) and plotted the cumulative distribution for each experimental group. Ocular dominance score was computed on cells with complete peristimulus time histogram analysis of peak and baseline spiking activity after closure of either eye. Ocular dominance score was defined as follows: {[peak(ipsilateral) − baseline(ipsilateral)] − [peak(contralateral) − baseline(contralateral)]}/{[peak(ipsilateral) − baseline(ipsilateral)] + [peak(contralateral) − baseline(contralateral)]}. This score is −1 for class 1 cells, +1 for class 7 cells, and 0 for class 4 cells.

Receptive field size. Receptive field size was measured on peristimulus time histograms evoked by stimulation of either eye with computer-generated bars of optimal orientation. The time during the sweep of the visual field at which spiking activity was above a baseline frequency of +2 SDs was measured. This time was then transformed in a visual angle, considering the velocity of drifting of the light bar.

Visual Acuity Assessment with VEPs. We measured visual acuity through both eyes with VEPs in the same electrode tracks where single-unit activity was acquired. To record VEPs, the electrode was positioned at a depth of 500 μm. Signals were band-pass-filtered (0.1–100 Hz), amplified, and fed to a computer for analysis as described previously (13). Briefly, at least 128 events were averaged in synchrony with the stimulus contrast reversal. Transient VEPs in response to abrupt contrast reversal (0.5 Hz) were evaluated in the time domain by measuring the peak-to-trough amplitude and peak latency of the major negative component. Visual stimuli were horizontal sinusoidal gratings of different spatial frequencies and contrast, generated by a VSG2/2 card running custom software and presented on a monitor (20×22 cm; luminance 15 cd/m^2) positioned 20 cm from the rat's eyes and centered on the previously determined receptive fields. Visual acuity was obtained by extrapolation to zero amplitude of the linear regression through the last four to five data points in a curve where VEP amplitude (normalized to the value recorded for the lowest spatial frequency used, 0.2 cycle/°) is plotted against log spatial frequency (13).

Behavioral Assessment of Visual Acuity. Visual acuity was determined by following the method of Prusky *et al.* (11). Briefly, adult long-term MD rats were reverse-sutured and assigned to the control group (two untreated rats and two rats treated bilaterally with P-ase) or to the group treated with chABC (four rats). The apparatus consists of a Plexiglas box filled with water, partially divided at one end in two arms by a divider. Visual stimuli, which are generated on computer monitors, are at the end of each arm. Stimuli consisted of gratings of various spatial frequencies or gray fields. The rat was placed at the nondivided end of the box and swam looking for the submerged platform corresponding to the grating. Grating and gray-field positions are alternated by following a pseudorandom sequence. The

visual water task trains animals to first distinguish a low (0.1 cycle/°) spatial-frequency grating. After the association between the submerged platform and the grating is formed, the spatial frequency of gratings is progressively increased. Visual acuity has been taken as the spatial frequency corresponding to 70% correct choices on the sigmoidal function fitting the psychometric function. For each animal, visual acuity of the nondeprived eye has been measured before treatment, whereas visual acuity of the other eye has been assessed after the reverse suture and chABC or P-ase treatment. During each session, the experimenter was blind to the experimental group.

Dendritic Spine Analysis. Spine density measurements were performed by using the protocol of Mataga *et al.* (4), with minor modifications. Twenty rats were used. Fourteen rats were control subjects (six RS rats, four RS rats treated with P-ase, and four RS rats treated with chABC with binocular vision), and six were RS chABC-treated animals. After decapitation, the brain was rapidly removed and immersed in ice-cold cutting solution containing 130 mM NaCl, 3.1 mM KCl, 1.0 mM K_2HPO_4, 4.0 mM $NaHCO_3$, 5.0 mM dextrose, 2.0 mM $MgCl_2$, 1.0 mM $CaCl_2$, 10 mM Hepes, 1.0 mM ascorbic acid, 0.5 mM myo-inositol, and 2 mM pyruvic acid (pH 7.3). A block of visual cortex was sectioned in the coronal plane into 300-μm-thick slices by using a vibratome (Leica, Vienna, Austria). The slices were transferred to a storage box containing cutting solution and maintained with oxygen at room temperature. Lipophilic dye (1,1′-dioctadecyl-3,3,3′,3′-tetramethylindocarbocyanine; Molecular Probes) was coated onto tungsten particles (diameter, 1.3 μm; Bio-Rad) according to Gan *et al.* (23). 1,1′-Dioctadecyl-3,3,3′,3′-tetramethylindocarbocyanine-coated particles were delivered to the slices by using a Helios Gene Gun System (Bio-Rad). A polycarbonate filter with a 3.0-μm pore size (Molecular Probes) was inserted between the gun and the preparation on a platform to remove clusters of large particles. Density of labeling was controlled by gas pressure (80 psi of helium). After labeling, slices were fixed in 4% paraformaldehyde. A Fluoview (Olympus, Tokyo) confocal microscope (60× water immersion objective; numerical aperture, 0.9) was used to image the labeled structures (1.5× zoom). At least 5–15 labeled typical pyramidal neurons were randomly selected from layer II–III in the binocular zone of the visual cortex ipsilateral and contralateral to the long-term-deprived eye. Images of basal dendrites were acquired, stacked (0.8-μm step), and then analyzed with METAMORPH (Molecular Devices) blind to the treatment. All protrusions along each dendrite from the second order to the next (according to image size) were counted from the first dendritic branch [beginning at 26.2 μm (SD, 6.8) from the soma depending on primary dendrite morphology; length of analyzed segments, 31.9 μm (SD, 12)]. Dendritic protrusions were not classified by morphology (e.g., filopodia and spines) because of classification ambiguities in stacked 3D images.

This study was supported by university and research funds from the Italian Ministry for Education [Fondo per gli Investimenti della Ricerca di Base 2001 (to T.P. and L.M.) and Progetti di Rilevante Interesse Nazionale 2005 (to T.P., N.B., and L.M.)].

1. Mitchell, D. E. & MacKinnon, S. (2002) *Clin. Exp. Optom.* 85, 5–18.
2. Hubel, D. H. & Wiesel, T. N. (1970) *J. Physiol. (London)* **206,** 419–436.
3. Fagiolini, M., Pizzorusso, T., Berardi, N., Domenici, L. & Maffei, L. (1994) *Vision Res.* **34,** 709–720.
4. Mataga, N., Mizuguchi, Y. & Hensch, T. K. (2004) *Neuron* **44,** 1031–1041.
5. Oray, S., Majewska, A. & Sur, M. (2004) *Neuron* **44,** 1021–1030.
6. Liao, D. S., Krahe, T. E., Prusky, G. T., Medina, A. E. & Ramoa, A. S. (2004) *J. Neurophysiol.* **92,** 2113–2121.
7. Blakemore, C., Vital-Durand, F. & Garey, L. J. (1981) *Proc. R. Soc. London Ser. B* **213,** 399–423.
8. Blakemore, C. & Van Sluyters, R. C. (1974) *J. Physiol. (London)* **237,** 195–216.
9. Kind, P. C., Mitchell, D. E., Ahmed, B., Blakemore, C., Bonhoeffer, T. & Sengpiel, F. (2002) *Nature* **416,** 430–433.
10. Mitchell, D. E. (1988) *J. Physiol. (London)* **395,** 639–660.
11. Prusky, G. T., West, P. W. & Douglas, R. M. (2000) *Eur. J. Neurosci.* **12,** 3781–3786.
12. Berardi, N., Pizzorusso, T., Ratto, G. M. & Maffei, L. (2003) *Trends Neurosci.* **26,** 369–378.
13. Huang, Z. J., Kirkwood, A., Pizzorusso, T., Porciatti, V., Morales, B., Bear, M. F., Maffei, L. & Tonegawa, S. (1999) *Cell* **98,** 739–755.
14. Hensch, T. K., Fagiolini, M., Mataga, N., Stryker, M. P., Baekkeskov, S. & Kash, S. F. (1998) *Science* **282,** 1504–1508.
15. Hockfield, S., Kalb, R. G., Zaremba, S. & Fryer, H. (1990) *Cold Spring Harbor Symp. Quant. Biol.* **55,** 505–514.
16. McGee, A. W., Yang, Y., Fischer, Q. S., Daw, N. W. & Strittmatter, S. M. (2005) *Science* **309,** 2222–2226.
17. Pizzorusso, T., Medini, P., Berardi, N., Chierzi, S., Fawcett, J. W. & Maffei, L. (2002) *Science* **298,** 1248–1251.
18. Pizzorusso, T., Fagiolini, M., Porciatti, V. & Maffei, L. (1997) *Vision Res.* **37,** 389–395.
19. Domenici, L., Berardi, N., Carmignoto, G., Vantini, G. & Maffei, L. (1991) *Proc. Natl. Acad. Sci. USA* **88,** 8811–8815.
20. Movshon, J. A., Eggers, H. M., Gizzi, M. S., Hendrickson, A. E., Kiorpes, L. & Boothe, R. G. (1987) *J. Neurosci.* **7,** 1340–1351.
21. Valverde, F. (1967) *Exp. Brain Res.* **3,** 337–352.
22. Wallace, W. & Bear, M. F. (2004) *J. Neurosci.* **24,** 6928–6938.
23. Gan, W. B., Grutzendler, J., Wong, W. T., Wong, R. O. & Lichtman, J. W. (2000) *Neuron* **27,** 219–225.
24. Sawtell, N. B., Frenkel, M. Y., Philpot, B. D., Nakazawa, K., Tonegawa, S. & Bear, M. F. (2003) *Neuron* **38,** 977–985.
25. Grutzendler, J., Kasthuri, N. & Gan, W. B. (2002) *Nature* **420,** 812–816.
26. Holtmaat, A. J., Trachtenberg, J. T., Wilbrecht, L., Shepherd, G. M., Zhang, X., Knott, G. W. & Svoboda, K. (2005) *Neuron* **45,** 279–291.
27. Konur, S. & Yuste, R. (2004) *J. Neurobiol.* **59,** 236–246.
28. Majewska, A. & Sur, M. (2003) *Proc. Natl. Acad. Sci. USA* **100,** 16024–16029.
29. Fawcett, J. W. & Asher, R. A. (1999) *Brain Res. Bull.* **49,** 377–391.
30. Silver, J. & Miller, J. H. (2004) *Nat. Rev. Neurosci.* **5,** 146–156.
31. Wegner, F., Hartig, W., Bringmann, A., Grosche, J., Wohlfarth, K., Zuschratter, W. & Bruckner, G. (2003) *Exp. Neurol.* **184,** 705–714.
32. Hartig, W., Brauer, K. & Bruckner, G. (1992) *NeuroReport* **3,** 869–872.
33. Fagiolini, M., Fritschy, J. M., Low, K., Mohler, H., Rudolph, U. & Hensch, T. K. (2004) *Science* **303,** 1681–1683.
34. Hensch, T. K. (2005) *Nat. Rev. Neurosci.* **6,** 877–888.
35. Bradbury, E. J., Moon, L. D., Popat, R. J., King, V. R., Bennett, G. S., Patel, P. N., Fawcett, J. W. & McMahon, S. B. (2002) *Nature* **416,** 636–640.
36. Bruckner, G., Bringmann, A., Hartig, W., Koppe, G., Delpech, B. & Brauer, K. (1998) *Exp. Brain Res.* **121,** 300–310.
37. Rittenhouse, C. D., Shouval, H. Z., Paradiso, M. A. & Bear, M. F. (1999) *Nature* **397,** 347–350.